Nanotoxicology, December 2011; 5(4): 687–699

informa
healthcare

Measurement of airborne nanoparticle surface area using a filter-based gas adsorption method for inhalation toxicology experiments

RYAN F. LEBOUF, ALEKSANDR B. STEFANIAK, BEAN T. CHEN, DAVID G. FRAZER, & M. ABBAS VIRJI

National Institute for Occupational Safety and Health, Centers for Disease Control and Prevention, Morgantown, West Virginia 26505, USA

(Received 4 October 2010; accepted 7 December 2010)

Abstract

Measurement of the surface area of airborne nanoparticles as administered to an experimental subject is critical for characterizing exposures during inhalation experiments. A filter-based surface area measurement methodology is described herein that allows for such determinations. Krypton gas adsorption was used to determine total particle surface area. Track-etched polycarbonate 0.4 μm pore filters were chosen as the collection substrate for metal oxide particles due to their highly reproducible surface areas and low background weights. The subject nanomaterials included two different batches of ultrafine TiO_2, TiO_2 nanorods, and SiO_2. The instrument detection limit for surface area was 200 cm^2 (0.02 m^2). Ninety percent confidence interval estimates of method accuracy were 17.7–23.5% with a point estimate of 20.8%. The filter-based surface area measurement strategy is demonstrated to be a viable sampling and analysis methodology that provides much needed physical characterization information of particles as administered in an animal inhalation chamber.

Keywords: *Nanoparticles, surface area, ultrafine titanium dioxide, sampling methodology*

Introduction

Accurate characterization of the physicochemical properties of an engineered nanomaterial (EN) defined as a material designed and produced to have structural features with at least one dimension <100 nm, is paramount for elucidating toxicologically-relevant dose metrics (Hansen et al. 2007; Hansen et al. 2008; Seaton et al. 2010). Material characteristics that may be important parameters for estimating the hazard of EN include chemical composition, size, shape, crystal structure, surface area, surface chemistry, surface charge, solubility, and adhesion (Hansen et al. 2007). Oberdörster et al. (2005) suggest a framework for characterization of EN for inhalation toxicology studies that includes:

- *As produced* (i.e., measured as the bulk material sold by the supplier),
- *As administered* (i.e., measured at the point of delivery to a test subject), and
- *After administration* (i.e., measured at the target organ *in vivo*).

Characterization following administration would be ideal due to potential changes during delivery such as aggregation or surface binding with proteins *in vivo*, but such measurements are currently difficult if not impossible to obtain (Oberdörster et al. 2005; Dwivedi et al. 2009). Characterization of a material 'as produced' provides baseline data on the physicochemical properties of the material provided by the supplier. During the delivery of an EN to a test subject, the material properties may undergo change and therefore have properties that differ from the material 'as produced'. The tiered strategy for EN characterization suggested by Oberdörster et al. (2005) may provide toxicologists with the needed information to draw meaningful conclusions concerning dose-response relationships. The goal of the current project was to develop a standard protocol for assessing the surface area of metal and oxide EN 'as produced' and 'as administered' in inhalation exposure chambers.

Surface area may be a key particle exposure property (Donaldson et al. 2000; Duffin et al. 2002; Stoeger et al. 2006; Monteiller et al. 2007;

Correspondence: Ryan F. LeBouf, PhD, National Institute for Occupational Safety and Health, Centers for Disease Control and Prevention, Morgantown, WV 26505, USA. E-mail: rlebouf@cdc.gov

ISSN 1743-5390 print/ISSN 1743-5404 online © 2011 Informa UK, Ltd.
DOI: 10.3109/17435390.2010.546951

Bello et al. 2009; Hussain et al. 2009; Seaton et al. 2010). Surface area of EN has been well correlated with decreased pulmonary function *in vivo* as well as an increase in oxidative stress and production of reactive oxygen species *in vitro* (Singh et al. 2007; Nurkiewicz et al. 2009; LeBlanc et al. 2010). Titanium dioxide (TiO_2) nanoparticles can trigger a pro-inflammatory response presumably due to their large surface area even though uptake in lung epithelial cells occurs as aggregates (Singh et al. 2007). Ferin et al. (1992) observed an increase in rat lung inflammation from ultrafine titanium dioxide ($uTiO_2$) particles compared to fine TiO_2 particles on a similar mass concentration basis. Donaldson et al. (2000) observed an increase in inflammatory response *in vitro* from ultrafine particles with a similar mass basis to fine particles of the same type. These researchers concluded that particle number or surface area was very likely responsible for the observed adverse effect.

Particle surface area can be delineated into internal surface area, external surface area, and total surface area. Internal surface area is the surface attributable to pore walls. Pores can be defined as cavities, channels or interstices having a depth greater than the width. External surface area is the area of the external surface of the particles, taking into account their roughness, i.e., all cavities which have a width greater than the depth, but not the surface of the pore walls. Total surface area is defined as the accessible area of all real particle surfaces. Estimates of particle surface area are commonly made from the following: (1) Determinations using geometric relations with external particle dimensions, (2) direct measurements using gas adsorption, (3) using electromobility properties of particles, or (4) ion attachment techniques (Rothenberger 1980; Stefaniak et al. 2003; Ku and Maynard 2005; Weibel et al. 2005). The surface area value determined by each of these types of methods depends upon the morphological characteristics of the material of interest. External dimensions of particles can be measured directly using electron microscopy or determined indirectly using particle size-selective samplers (e.g., inertial impactors). Use of geometric relations between particle external dimension and surface area is only appropriate for smooth regularly shaped compact particles (Stefaniak et al. 2003; Weibel et al. 2005). Weibel et al. (2005), for example, report that estimates of $uTiO_2$ surface area determined using a geometric relationship with physical particle size (determined using transmission electron microscopy) were 50% lower than measured directly using nitrogen gas adsorption due to the presence of mesopores. Direct measurement methods include adsorption of gas to particle surfaces using the Brunauer, Emmett, and Teller (BET) method or, alternatively, attachment of charged ions to particle surfaces using diffusion chargers. Gas adsorption provides an estimate of total particle surface area and has historically been used for bulk (gram) quantities of material 'as produced'. Diffusion chargers provide an estimate of airborne particle external surface area from microgram quantities of material with particle sizes smaller than 100 nm in diameter (Ku and Maynard 2005).

For this study, we used a filter-based method of particle collection followed by gas adsorption to determine surface area of airborne metal and metal oxide particles from an animal inhalation exposure chamber. $uTiO_2$ was chosen as a model material due to its prevalence and use in industrial applications as well as toxicological research. The specific aims of this study were to: (1) Develop a framework for selection of an appropriate filter media with low background surface area and high weight stability; (2) determine analytical limits of detection and quantification for the gas adsorption instrument and evaluate response linearity; (3) characterize a commercially-available bulk $uTiO_2$ powder 'as produced' (i.e., predicted surface area) for use as a model test material; (4) determine the 'as administered' (i.e., measured) surface area of the airborne model $uTiO_2$ material; and (5) verify method performance and generalizability by determining the 'as administered' surface area of a second airborne $uTiO_2$ powder, TiO_2 nanorods, and silicon dioxide EN collected on filter media in a laboratory inhalation exposure chamber.

Materials and methods

Filter selection framework

The background characteristics of an air sampling filter will influence the reproducibility and limit the sensitivity of surface area measurements of airborne (as administered) nanoparticles collected onto the filter for gas adsorption analysis. The focus of the current research is metal and metal oxide EN, though the same filter evaluation strategy applies for other types of nanomaterials such as carbon nanotubes, etc. Key filter evaluation criteria are:

- Highly reproducible and low background weight (to permit gravimetric determination of sample mass);
- Highly reproducible and low surface area (influences the analytical limit of detection);
- Low pressure drop (to permit collection of air samples for a sufficient duration to exceed analytical detection limits);
- High collection efficiency (in the particle size range of interest); and
- Preservation of physical integrity (under particle degas temperature conditions).

For the purposes of this method development study, two substrate materials were evaluated, 5 μm pore size polytetrafluoroethylene (PTFE) membrane (Teflon®) filters (SKC Inc., Eighty Four, PA, USA) and 0.4 μm and 0.8 μm pore size Nucleopore® track-etched polycarbonate (TEPC) filters (Sterlitech Corporation, Kent, WA, USA). PTFE filters were selected based on weight stability and low background surface area data previously published (Sheffield and Pankow 1994). TEPC filters were selected because they have limited sensitivity to relative humidity (RH), which significantly reduces the requirements for special humidity-controlled chambers for conditioning filters prior to weighing (Lawless and Rodes 1999). Additionally, both types of filters are available in a range of diameters, typically from 25–47 mm, that will accommodate various air sampling heads and are also available in several pore sizes.

Background weight stability

Prior to measuring surface area by gas adsorption, samples are conditioned (degassed) to remove physisorbed material such as water from the surface. In our experience, metal oxides require 4 h to fully degas at 200°C (Stefaniak et al. 2003). PTFE and TEPC filters have maximum working temperatures of 140–150°C. Background filter weight (i.e., $Mass_b$) was measured gravimetrically by recording triplicate readings using a calibrated electronic microbalance (Model UMX2, Mettler Toledo, Greifensee, Switzerland) capable of reading to 10 μg (i.e., five-place balance). All filters were pre-conditioned for 24 h in a temperature (19.7 ± 0.8°C) and humidity (46.7 ± 8.0% RH) controlled chamber (Nor-Lake, Inc., Hudson, WI, USA) before weighing. Each filter was handled on the edges only using metal tweezers and passed though a U-shaped static charge neutralizer (Haug GMBH + Co. KG, Germany) before weighing. Five filters of each type were degassed at three different temperatures (no heat, 60°C, or 120°C) for two different durations (6 or 24 h). Each filter was pre-weighed at three separate times on two different days before exposure, degassed, and post-weighed in the same manner.

Background surface area stability

Each filter type was degassed under light vacuum (P ~ 0.015 Torr; Flovac™ Degasser, Product No. 05076, Quantachrome Instruments, Boynton Beach, FL, USA) at two different temperatures (60°C, or 120°C) for two different durations (6 or 24 h) to identify preparation conditions that would provide a stable measure of background surface area while preserving the physical integrity of the substrate. A control condition of no heat for both 6 and 24 h was performed for the TEPC 0.4 μm filter. Each blank filter was loaded into a pre-weighed and pre-calibrated 9-mm glass sample cell (part no. 74099, Quantachrome Instruments) and background surface area determined by krypton gas adsorption using the BET method. Filter surface area measured with a Quadrasorb-*SI* (Quantachrome Instruments) was estimated from seven point adsorption isotherms collected at relative pressures in the range p/p_0 = 0.05–0.35; a value of 20.5 $Å^2$ was assumed for the cross-sectional area of a krypton molecule. Due to the expected low surface area of the filters and samples, krypton rather than nitrogen was chosen as the adsorbate. At low surface areas, the amount of nitrogen gas remaining in the sample cell void volume becomes increasingly large relative to the amount that is actually adsorbed to the sample which can result in large measurement error. In contrast, krypton gas has lower saturation vapor pressure than nitrogen at 77 K, meaning that less gas will remain in the void volume. Instrument settings were: 1 min equilibration time and 0.05 pressure tolerance. Typical analysis time after degassing was approximately 100 min. A TiO_2 powder (SRM 2001, Quantachrome Instruments) with assigned specific surface area (SSA) of 8.46 ± 0.9 m^2/g was used as a reference standard and analyzed in parallel with filter samples periodically throughout the study; the average measured SSA for this control sample was 8.44 ± 0.41 m^2/g.

Four filters of each type were exposed to each degas temperature and duration. Duplicate measures of surface area (SA) were performed on each filter at each temperature/time condition. The SA is merely the SSA times the mass. The sample size per condition was based on 80% statistical power to detect 10% change in surface area between two conditions at a significance level of 0.05.

Filter pressure drop, collection efficiency, and physical integrity

To evaluate the feasibility of using PTFE and TEPC filters for long-term (i.e., hours) sampling during inhalation exposure studies, the pressure drop across each filter (n = 6 filters of each type) was evaluated before and after degassing at the same temperature and time combinations as was performed for weight stability and surface area determinations.

The collection efficiency of each filter type (n = 7 filters of each type) was determined using a

CertiTest® Model 3160 Automated Filter Tester (TSI, Inc., Shoreview, MN, USA). Collection efficiency was measured at five different challenge concentrations of monodisperse sodium chloride aerosol with sizes between 20 and 100 nm, inclusive, at 2 L/min flow rate. Percent collection efficiency was calculated from the difference between upstream and downstream measurements from a condensation particle counter.

Finally, a subset of each filter type was inspected by scanning electron microscopy (S-4800 Field Emission SEM, Hitachi, Tokyo, Japan) before and after degassing to inspect the physical integrity of the media for signs of damage from heating. All of these parameters must be evaluated since the filter underwent background surface area measurements prior to sample loading.

Instrument detection limits and response linearity

Measurements of background filter surface area yielded an expected instrument limit of detection (LOD) of 250 cm^2 for 37-mm, 0.4 μm pore size TEPC filters. The protocol described by Kennedy et al. (1995) was used to determine the actual LOD, defined as the mass of analyte which gives a mean signal three times the standard deviation above the mean blank signal (σ_b). The limit of quantification (LOQ) is defined as the lowest mass of analyte that can be reported with acceptable precision and is equivalent to 3.33·LOD or the mass above which recovery is ≥75% (Kennedy et al. 1995).

For the purposes of our study, we used $n = 7$ low-level calibration spikes to determine the LOD. An aluminum oxide certified reference material (CRM), BAM-PM-104, with surface area of 79.8 ± 0.4 m^2/g (Federal Institute for Materials Research and Testing, Berlin, Germany) was used to determine the LOD and assess linearity of the instrument response. The nominal distribution of the seven standards was as follows: Three standards slightly below the expected LOD (100 $cm^2 \equiv 0.1253$ mg; 150 $cm^2 \equiv 0.1880$ mg; 200 $cm^2 \equiv 0.2506$ mg), one mass at five times the LOD (1100 $cm^2 \equiv 1.3784$ mg), and three masses at 10 times the LOD (1760 $cm^2 \equiv 2.2055$ mg; 2200 $cm^2 \equiv 2.7569$ mg; 2640 $cm^2 \equiv 3.3083$ mg). To evaluate linearity, filters were inoculated with nominal masses of CRM equivalent to surface areas of 200 (0.25 mg), 400 (0.5 mg), 800 (1 mg), 2400 (3 mg), and 4000 cm^2 (5 mg). The masses for estimating the detection limits and linearity were selected to be within mass concentrations to which humans in the work environment (Fryzek et al. 2003) and animals in toxicological assessments (Lee et al. 1985a, 1985b, 1986; Bermudez et al. 2004) have been exposed.

The masses for estimating the LOD/LOQ and linearity were selected based on mass concentrations to which humans in the work environment and animals in toxicological assessments have been exposed. Fryzek et al. (2003) investigated cancer mortality among workers at plants producing pigment grade TiO_2. While the authors did not mention particle size distribution, it is assumed from the process descriptions that the dust was polydisperse with a modal diameter in the fine region (nominal particle modal diameter > 100 nm). The authors reported that from 1976–2000 exposure levels decreased in four manufacturing facilities in the United States. In the period 1996–2000, the average exposure level among the four facilities was 3.1 mg/m^3 with median 1.1 mg/m^3 and geometric mean (GM) 1.0 mg/m^3. Among jobs, packers/micronizers/and addbacks had the highest exposures (mean 6.2 mg/m^3, median 3.0 mg/m^3, GM 2.7 mg/m^3) and dry and wet treatment workers were among the lowest (mean 2.0 mg/m^3, median 0.3 mg/m^3, GM 0.4 mg/m^3). As these exposure levels were calculated from full-shift lapel samples, the volume of air sampled was presumed to be approximately 1 m^3 which corresponds to sample masses of up to 6 mg. In another cancer mortality study, Boffetta et al. (2004) reported similar exposure concentrations among European TiO_2 pigment production workers.

Limited animal inhalation exposure data exists to supplement this human exposure data. Lee et al. (1985a, 1985b, 1986) and Trochimowicz et al. (1988) reported results from a two-year rat inhalation study in which animals were exposed to fine TiO_2 for 6 h per day, five days per week at 10 mg/m^3, 50 mg/m^3, and 250 mg/m^3. In these studies, fine TiO_2 was used with a mass median aerodynamic diameter between 1.5 and 1.7 μm; approximately 80–90% of the dust was respirable size. More recently, Bermudez et al. (2004) reported a subchronic inhalation study in which female rats, mice, and hamsters were exposed to Degussa P25 uTiO_2 (average primary particle size of 21 nm) for 6 h per day, five days per week, over 13 weeks at aerosol concentrations of 0.5 mg/m^3, 2.0 mg/m^3, or 10 mg/m^3.

Characterization of study powders

A commercially available uTiO_2 material (Product Type P25, Degussa AG, Hanau, Germany) was chosen for use as a model material because it: (1) Represents a widely studied powder often used in toxicological investigations (Maier et al. 2006), and (2) this material is being qualified by the U.S. National Institute of Standards and Technology (NIST) as a certified reference material. A suite of analytical techniques was used to characterize

the physicochemical properties of a bulk P25 $uTiO_2$ powder 'as produced'. Transmission electron microscopy (TEM) was used to evaluate the morphology and size of particles; energy dispersive X-ray spectrometry (TEM-EDS) to determine elemental constituents; X-ray diffraction (XRD) to identify crystalline constituents and also quantify the abundance of those phases (e.g., using Rietveld Refinement techniques); X-ray photoelectron spectroscopy to evaluate surface chemistry; helium pycnometry (Multipycnometer, Quantachrome Instruments) to determine material density; and nitrogen gas adsorption (Nova 2200e, Quantachrome Instruments) to determine surface area.

Additionally, a second P25 $uTiO_2$ powder (Degussa) previously used in a rat inhalation study (Nurkiewicz et al. 2009; Scuri et al. 2010), TiO_2 nanorods (5480MR, Titanium oxide (Rutile), 10×40 nm, 99.95%, Nanostructured & Amorphous Materials, Inc., Houston, TX, USA), and nanosilicon dioxide (Cat.# 637238-250G, 15 nm, 99.5%, Sigma-Aldrich Corp., St Louis, MO, USA) were used to confirm efficacy of the sampling strategy for a range of materials. The second P25 $uTiO_2$ powder was from another lot. These powders were characterized using TEM to evaluate morphology and size and krypton gas adsorption to determine the 'as produced' surface area of the materials.

Surface area of aerosolized nanoparticles in an inhalation chamber

Laboratory chamber studies were conducted to demonstrate the use of this method to measure 'as administered' nanoparticle surface area using 37-mm close-faced cassette samplers. To simulate an animal inhalation experiment, the model $uTiO_2$ powder was aerosolized in a well characterized laboratory system (Chen et al. 2006). The system is comprised of a fluidized-bed powder generator, plenum, static discharge device, and a fan at the entrance of the chamber to provide good mixing for the aerosol so that it has a homogenous concentration in the chamber. A single port in the chamber allows access by several aerosol monitoring devices. The filters were collected outside the chamber from the sampling port that was split with a Y-connector to two filter cassettes.

To reduce the potential formation of aggregates due to van der Waals force, the $uTiO_2$ powders were carefully prepared for generation by sieving (to remove the big aggregates), drying (to avoid aggregate formation due to high humidity), and storage (to prevent aggregate attraction through contact charges). The fluidized-bed aerosol generator with a cyclone was operated at a flow rate of 10–12 L/min to disperse $uTiO_2$ powders effectively. A 19-L metabolism plenum was modified for use as the aerosol chamber. During sampling, $uTiO_2$ mass concentrations were continuously monitored with a Data RAM (DR-4000 Thermo Electron Co, Franklin, MA, USA) and gravimetrically measured with Teflon filters. An aerosol concentration around 6 mg/m^3 was achieved by adjusting the powder feed rate in the generator. In addition, temperature, relative humidity, and pressure in the chamber were monitored throughout the sampling.

Background filter weight was determined gravimetrically and background filter surface area determined by krypton gas adsorption as described previously. To collect sufficient 'as administered' $uTiO_2$ surface area on filter samples to exceed the expected method LOD (250 cm^2 – see *Results*), a chamber concentration of 6 mg/m^3 was sampled at 3 L/min for varying durations to achieve six different filter surface area loadings (167 cm^2 = 325 μg, 304 cm^2 = 591 μg, 538 cm^2 = 1044 μg, 727 cm^2 = 1412 μg, 951 cm^2 = 1846 μg, and 1159 cm^2 = 2250 μg); two samples were collected simultaneously per surface area loading. The second P25 TiO_2 was aerosolized and sampled under the same conditions to confirm the results obtained with the well-characterized model powder. Both $uTiO_2$ powders were sieved and dried prior to aerosolization while the TiO_2 nanorods and nanosilica powders were not.

The TiO_2 nanorods and nanosilica powders were aerosolized using a Venturi disperser (In-Tox Products, Moriarty, NM, USA). An air flow of 20 L/min was introduced through the Venturi to disperse the powders as aerosol into the chamber and then collected onto filters at a flow rate of 2 L/min. The excess flow was connected to a vacuum line so that the chamber pressure was maintained slightly below ambient. Two samples were collected in replicate at four different loadings for a total of $n = 8$ samples per material. After collection, each nanoparticle particle-laden filter was degassed at 120°C for 24 h and total (filter + particle) surface area determined using krypton gas adsorption; the 'as administered' nanoparticle surface area was determined by subtracting the background filter surface area from the total measured surface area.

The SA of the particulate on a filter is given by Equation 1:

$$SA = (SSA_s \cdot Mass_s) - (SSA_b \cdot Mass_b)$$

where, SA = surface area of sample (m^2)

SSA_s = specific surface area of sample (m^2/*g*)

SSA_b = specific surface area of blank (m^2/*g*)

$Mass_s$ = mass of sample (*g*)

$Mass_b$ = mass of blank (*g*) (1)

background filter weight and surface area. Multiple comparisons of differences between means among filter types and conditions were conducted in the MIXED procedure using the LSMEANS statement with Tukey's option in SAS. The MIXED procedure is a modeling approach that allows for both random and fixed effects to be incorporated as covariates in the assessment of variables. The LSMEANS statement refers to least-squares means of the fixed effect. The Tukey's option allows for comparison of the LSMEANS between subjects to identify statistically significant differences. Since these measurements were made in duplicate, estimates of within and between filter variations in mass and surface area for the different filter types and the varying conditions were obtained from the repeated measurements.

To assess the LOD and linearity of the surface area instrument, linear regression models were fitted to measured values of surface area for the spike samples; regression plots were generated and regression parameters estimated using Sigmaplot 9.0 (Systat Software, Inc., Chicago, IL, USA). Estimates of analytical method precision, bias, and accuracy for surface area were determined using the method described by Kennedy et al. (1995). Briefly, precision was estimated by the coefficient of variation (CV) of the surface area ($CV = \sigma/\mu$) measurements at each mass loading. Bartlett's test was used to evaluate the homogeneity of precision across different loadings and calculate a pooled CV (if precision is constant). Bias was measured as the ratio of the mean measured surface area to the predicted surface area minus one at each loading level. The homogeneity of bias across the range of loadings was not tested since the number of generations was less than one. Accuracy was determined by calculating 90% two-sided confidence interval around the estimate of accuracy. Accuracy calculations were compared with a secondary assessment method based on Bartley (2001), which is an approximated computational method.

Linear and orthogonal regressions as well as paired t-tests were used to examine the agreement between measured SA and that predicted from the bulk powder material. Linear and orthogonal regressions were prepared in JMP 8.0 (SAS Institute), which is a graphic-user-interface based statistical package.

Results

Background weight stability

As illustrated in Figure 1, TEPC 0.8 μm pore filters had the lowest and most stable background mass. For the 0.4 μm pore TEPC filters, a statistically significant difference was observed between the control (i.e., no heat and light vacuum) mass and degassed mass for all combinations of temperature and time as indicated by the asterisks in Figure 1. A comparison between degas conditions, indicated by letters in Figure 1, showed that 6 h and 60°C was different from the other three conditions. PTFE filters had stable background weight, though the filter masses were a factor of 17 times higher than TEPC filters. As such, use of the PTFE filter type would necessitate collection of large masses of nanoparticles to permit gravimetric determination of sample mass; however, a more

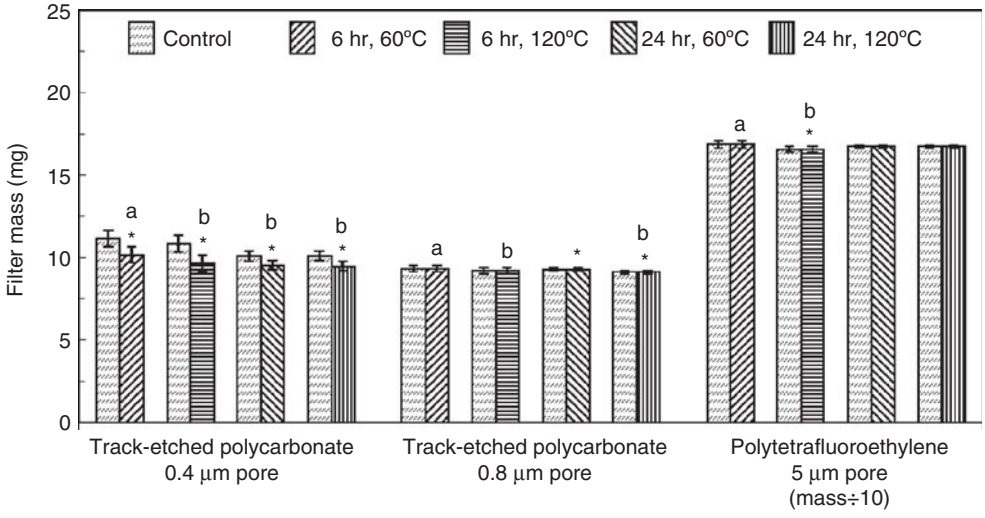

Figure 1. Average background mass of filter media by type and pre-conditioning parameters. Control = no heat and light vacuum for the duration of the given test condition. Error bars are 95% confidence intervals. * = statistical difference between pairs ($p < 0.05$); letter = statistical difference among conditions for a given filter type ($p < 0.05$). Note that the masses of PTFE filters were divided by 10 to allow plotting on the same y-axis scale as the TEPC filters.

sensitive method such as atomic spectroscopy could be used in lieu of weighing.

Background surface area stability

Figure 2 summarizes the background surface areas of the three different filter types. The TEPC 0.4 μm pore filters had the lowest and most stable background surface area. For this filter type, a statistical difference between degas conditions, indicated by letters in Figure 2, was observed between 6 h/60°C and 24 h/120°C. For this reason, all subsequent filters were degassed at 24 h/120°C. No statistical difference was observed for the 6 h/120°C and 24 h/60°C conditions. Relative to the TEPC 0.4 μm filters, the background surface areas of the PTFE and TEPC 0.8 μm filters were a factor of 3–4 times higher and more variable. A control condition of 6 and 24 h with no heat was conducted to determine whether heating had an influence on the background SA of the TEPC 0.4 μm filter only. No statistical difference was observed between 24 h with no heat, 24 h at 120°C and 6 h at 120°C. Results (not shown) indicated higher within filter variability than between filter variability; this means that an average background SA may be determined for a given filter lot and used instead of individual background measurements on each filter prior to loading.

Filter pressure drop, collection efficiency, and physical integrity

There was no statistical difference in pressure drop across the different filter types after degassing (data not shown). Visual inspection of a subset of filters using scanning electron microscopy did not reveal any alterations (e.g., cracks, distortions) in the filters after degassing (data not shown). The preservation of the filter media characteristics after degassing was quantitatively confirmed by measuring particle collection efficiency. As shown in Table I, the TEPC 0.4 μm pore filters had the highest particle collection efficiency in the range 20–100 nm at 2 L/min flow rate.

Instrument detection limit and response linearity

BET surface area instrument LOD was 200 cm^2 (0.02 m^2) based on a 0.005 standard error of estimate on the regression (R^2 = 0.986, slope = 0.975 and y-intercept = −0.001). Instrument LOQ was 510 cm^2 (0.051 m^2). Linearity regression values were as follows: R^2 = 0.947, slope = 1.000 and y-intercept = −0.025.

Pooled precision over ten mass loadings with two replicates per loading was 3%.

Bias was averaged across mass loadings to obtain an estimate of accuracy. Averaged bias value was −16% indicating an underestimation in measured SA based on predicted SA values. Using the Kennedy et al.

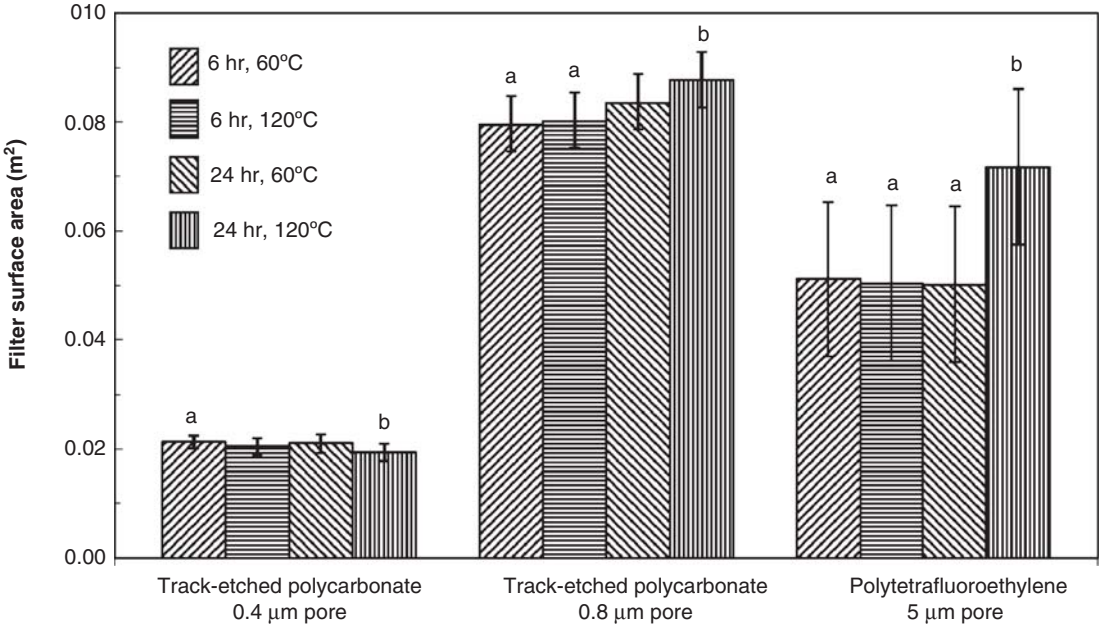

Figure 2. Average background surface area of filter media by type and pre-conditioning parameters. Error bars are 95% confidence intervals. Letter = statistical difference among conditions for a given filter type ($p < 0.05$).

Table I. Average collection efficiencies of filters (n = 7).

Filter	Pore (μm)	Avg ± SD collection efficiency (%)				
		20 nm	40 nm	60 nm	80 nm	100 nm
TEPC	0.4	99 ± 1	99 ± 2	98 ± 3	98 ± 3	97 ± 4
TEPC	0.8	99 ± 1	96 ± 1	94 ± 2	92 ± 2	91 ± 2
PTFE	5.0	94 ± 3	91 ± 4	90 ± 4	88 ± 7	87 ± 8

(1995) method, 90% confidence interval estimates of accuracy were 17.7–23.5% with a point estimate of 20.8%. Using the Bartley (2001) method, 90% confidence interval estimates of accuracy were 19.2–24.4% with a point estimate of 20.8%. The accuracy calculation methods compared well with each other. Since all values are below 25%, the method fulfills the 25% accuracy criterion as outlined in Kennedy et al. (1995).

Characteristics of study powders

A representative gas adsorption-desorption isotherm as well as a TEM image of particle morphology and size of the bulk (as produced) model P25 uTiO_2 powder (Batch 1) are presented in Figure 3. Consistent with published values for P25 uTiO_2 (Maier et al. 2006), the bulk powder was aggregate clusters of primary particles having GM diameter of 20 nm with geometric standard deviation (GSD) of 1.2; the GM cluster diameter was 67 nm with GSD of 1.7. Park et al. (2009) also reported a primary particle size of 20 nm for product type P25 powder. Powder density as measured by helium pycnometry was 3.76 ± 0.07 g/cm^3. The nitrogen gas adsorption/desorption isotherm exhibited a hysteresis loop that closes at p/p_0 = 0.3, indicative of mesopores and/or interparticle voids (see Figure 3). The pore volume of the material as determined using the Barrett-Joyner-Halenda method was 0.14 cm^3/g and the average pore diameter was 186 Å. The SSA of the bulk powder was 51.5 ± 0.2 m^2/g, which is in close agreement with the value of 50 m^2/g reported by Maier et al. (2006). Prior to aerosolization in the chamber studies (described below), the bulk powder was sieved and dried which reduced the SSA to 47.2 ± 1.5 m^2/g.

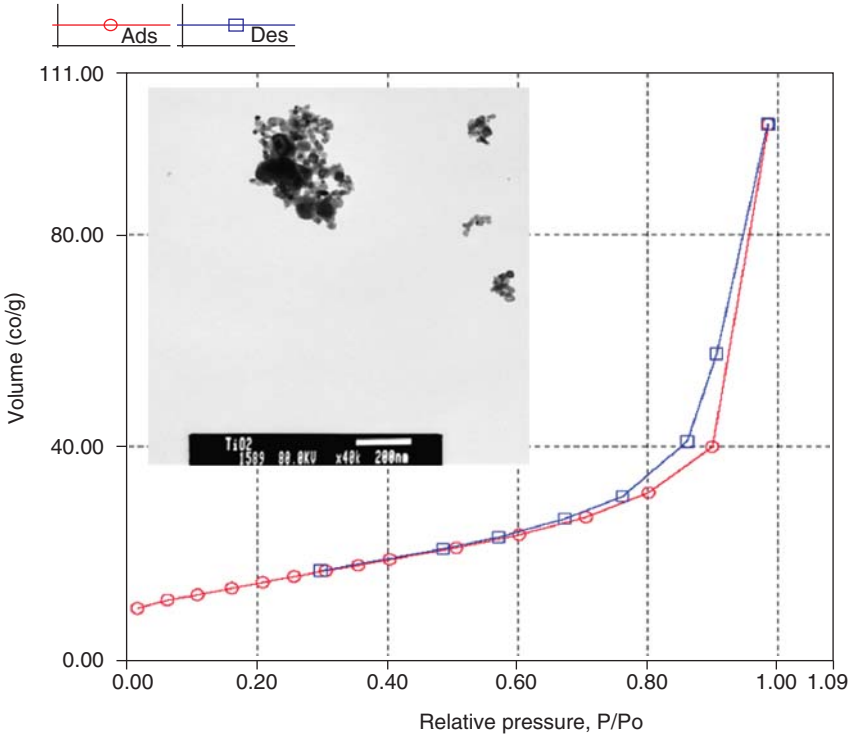

Figure 3. TEM image of bulk uTiO_2 Batch 1 powder and representative gas adsorption-desorption isotherm for surface area measurements; red line (circles) = adsorption, blue line (squares) = desorption.

According to the manufacturer, this material P25 powder is aggregate clusters of approximately 20 nm primary particles and consists of approximately 80% anatase phase TiO_2 and 20% rutile (Maier et al. 2006). Powder X-ray diffraction analysis revealed that the $uTiO_2$ powder was crystalline anatase (78%) and rutile (15%), which compares well with manufacturer specifications. Analysis of surface chemistry using X-ray photoelectron spectroscopy identified TiO_2 as the only oxidation state of Ti on powder surfaces; C, N, S, Ca, and Na were also detected.

The SSA of additional study powders were as follows: TiO_2 nanorods (160.4 ± 2.7 m^2/g) and SiO_2 nanoparticles (57.0 ± 4.9 m^2/g). Specific surface area of a second ultrafine TiO_2 (Batch 2) was measured with krypton: mean SSA is 53.6 ± 0.3 m^2/g. Upon sieving and drying the SSA was reduced to 48.4 ± 1.5 m^2/g. The morphology of TiO_2 nanorods, SiO_2 nanoparticles, and ultrafine TiO_2 Batch 2 can be seen in Figure 4. Agglomeration of primary particles is apparent in all three powders.

Surface area of aerosolized nanoparticles in an inhalation chamber

For a homogeneous exposure environment such as an inhalation exposure chamber, background filter surface area is the limiting characteristic for sensitivity of this method. Surface area of TEPC 0.4 μm pore filters (conditioned for 24 h at 120°C) were lowest among all filter media types evaluated and the calculated LOD for this filter was 0.025 m^2 of nanoparticle surface area, which compared well to the measured value of 0.02 m^2. For our model P25 powder, this LOD equals 0.49 mg of material, which is equivalent to the lowest mass concentration used in an $uTiO_2$ inhalation toxicology study (Bermudez et al. 2004). While pressure drop, collection efficiency and physical integrity of filter media were important evaluation metrics, highly reproducible and low background for both surface area and weight stability were the driving factors in the decision to use TEPC 0.4 μm pore filters.

Measured SA values of nanomaterial on filters were compared to predicted SA values calculated from the bulk material (SSA of sieved and dried $uTiO_2$ times mass used). Batch 1 measured SA values were slightly underestimated (orthogonal slope = 0.79). Predicted and measured SA values of $uTiO_2$ Batch 1 were statistically different based on a paired *t*-test ($p = <0.001$). Predicted and measured SA values of $uTiO_2$ Batch 2 compared well based on paired *t*-tests ($p = 0.664$) as well as linear and orthogonal regressions (Table II). Measured SA values for TiO_2 nanorods and SiO_2 nanoparticles loaded on filters were slightly underestimated. A statistical difference was observed between measured and predicted values for TiO_2 nanorods and SiO_2 nanoparticles ($p = 0.018$ and 0.004, respectively). A visual representation of the data scatter may be seen in the least-squares regression plots (Figure 5).

To determine whether the aerosolization method had an influence on SA measurements, Batch 2 TiO_2 was collected using the Venturi disperser. Batch 2 was chosen since it displayed the best correlation between measured and predicted SA values. Measured SA values were slightly underestimated (slope = 0.892, y-intercept = 0.0077, R^2 = 0.96) but not statistically different from the predicted values for $n = 4$ samples at four different loadings ($p = 0.070$). Aerosolization method does not appear to significantly affect measured SA values for nanomaterial collected on filter media, although it may have slightly contributed to the underestimation of TiO_2 nanorods and SiO_2 nanoparticles as can be seen from a reduction in slope from 0.985 (inhalation chamber) to 0.892 (Venturi disperser).

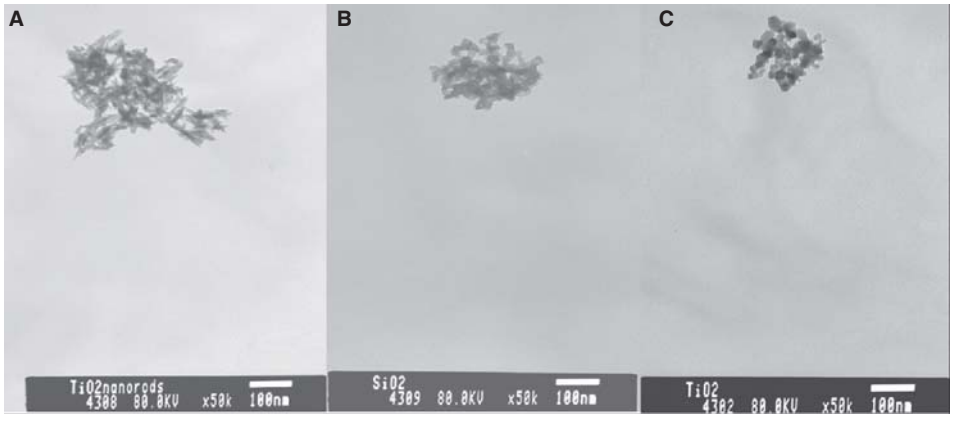

Figure 4. TEM image of bulk (A) TiO_2 nanorods, (B) SiO_2, and (C) $uTiO_2$ Batch 2 powder.

Table II. Paired *t*-tests ($\alpha = 0.05$) and regression values.

		Orthogonal			Least-squares		
Material	*p*-value	Slope	Intercept	R^2	Slope	Intercept	R^2
$uTiO_2$ Batch 1	<0.001	0.789	−0.0042	0.96	0.765	−0.0033	0.92
$uTiO_2$ Batch 2	0.664	0.985	0.0014	0.98	0.966	0.0023	0.96
TiO_2 nanorods	0.018	0.635	0.011	0.94	0.612	0.0147	0.88
SiO_2 nanoparticles	0.004	0.678	−0.0061	0.93	0.647	−0.0034	0.86

Discussion

The disagreement between measured and predicted SA values indicates that the 'as administered' differs from the 'as produced' particle SA; the 'as administered' value is preferable for toxicological studies (Oberdörster et al. 2005). The apparent difference between the measured and predicted SA values may have been due to the aerosolization of material. The predicted SA value was calculated using the gravimetrically determined mass of particles on the filter and the measured SSA of the sieved and dried bulk powder. During aerosolization, particles agglomerated which resulted in a polydisperse size distribution; this could reduce the observed SA values 'as administered'. The shift in airborne particle size distribution that was collected on filters versus the size distribution of the sieved and dried bulk powder may account for some of the observed difference in measured versus predicted SA values.

While the agreement between measured and predicted values was found to vary for different particles

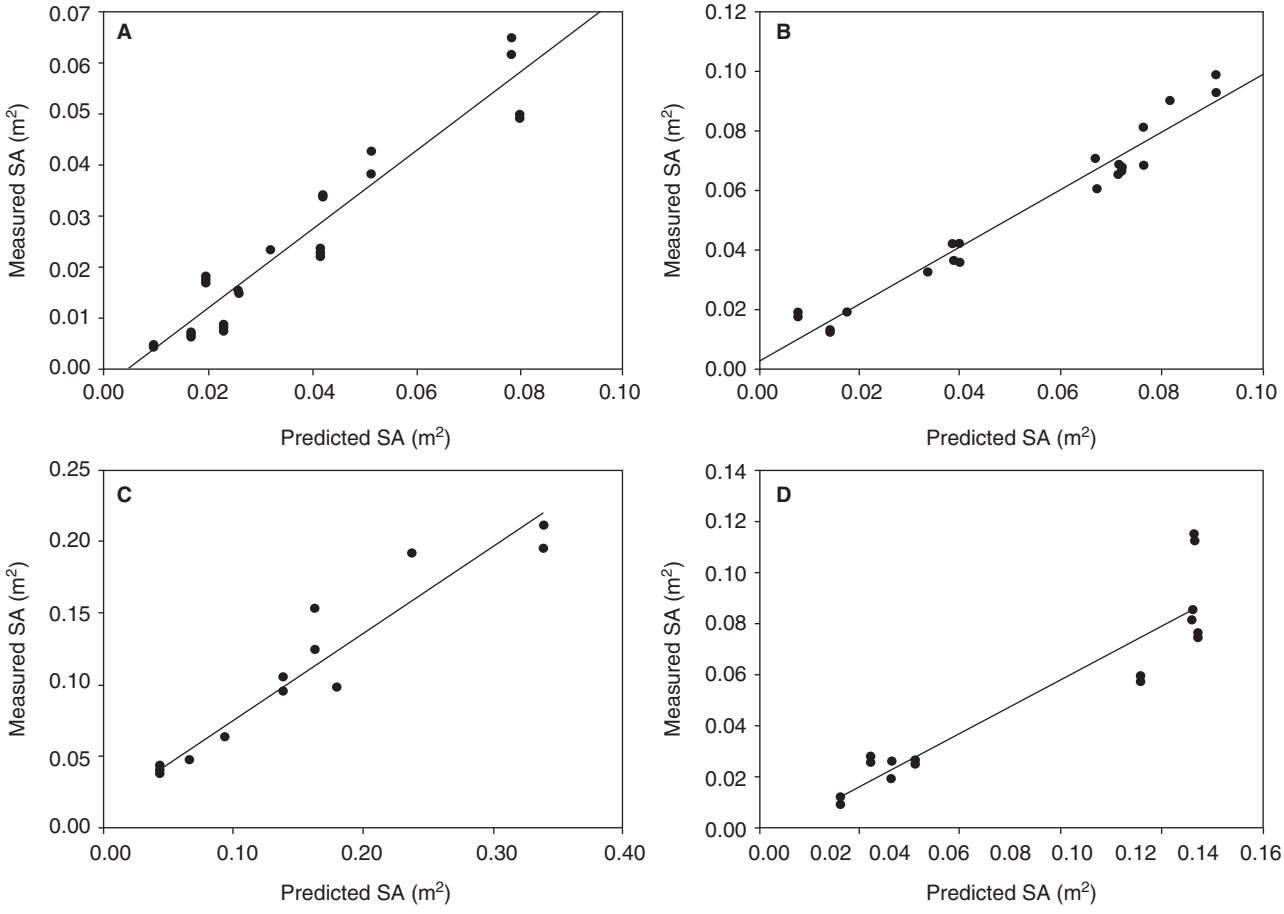

Figure 5. Linear regressions of measured versus predicted SA for (A) $uTiO_2$ Batch 1, (B) $uTiO_2$ Batch 2, (C) TiO_2 nanorods, and (D) SiO_2 nanoparticles.

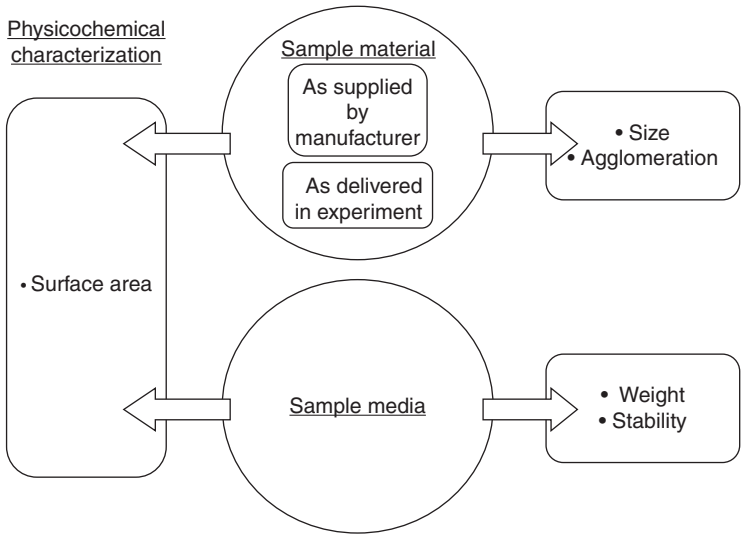

Figure 6. Nanomaterial characterization framework.

and collection techniques (i.e., inhalation chamber versus Venturi disperser), this preliminary work laid the foundation for further refinement of a filter-based SA measurement framework. In the future, the current study design could be modified to assess relative humidity and temperature effects; gravimetric TiO_2 content could be determined by mass spectrometric analysis; and SA results could be confirmed by a third-party analytical laboratory.

Advantages of this method include the following: Robustness – any sampler may be used with filter media that possesses low and stable surface area; adaptability – uses commercially available filter media for particle collection and established gas adsorption theory for surface area measurements; and versatility – the filter sample may be used in subsequent analyses such as electron microscopy, X-ray fluorescence (non-destructive), and/or inductively coupled plasma mass spectrometry (destructive) to provide additional information on the 'as administered' material. Gas adsorption measurement of particle SSA via BET method is favored over predictions from particle size when contributions from surface roughness, pores, or internal surface are significant (Rothenberger 1980; Stefaniak et al. 2003; Weibel et al. 2005). Surface area may provide the basis for a predictive testing system for nanoparticles that allows for the development of a robust exposure assessment strategy (Duffin et al. 2002; Stoeger et al. 2006).

Need for standard test methods

Occupational exposures to nanomaterials, during the production or use of the material, are becoming more prevalent due to a rise in nanotechnology development and implementation as can be seen from the Woodrow Wilson database of consumer products containing nanoparticles (Hansen et al. 2008; Seaton et al. 2010). Standardized test methods for occupational exposure to nanoparticles are currently lacking (Grieger et al. 2009). A sampling regime needs to be defined that effectively captures the physiologically relevant exposure parameters in a homogeneous manner so that comparisons can be made between toxicological and material research. A proposed strategy is outlined in Figure 6 that involves characterizing a nanomaterial *as produced* by the manufacturer and *as administered* to the target organism. Physicochemical characterization of the material includes the following: size, agglomeration, surface properties (area, charge, and chemistry). Physicochemical characterization of the sampling media involves surface area measurements and assessment of weight stability. The current research provides a means of evaluating nanomaterials using a filter-based collection strategy that would be more representative of actual exposure metrics at the point the material is received by the host organism in toxicological research or nanomaterial manufacturing facilities. The proposed filter characterization framework could be adapted for other forms of EN such as carbon nanotubes to provide a standard basis for comparison across toxicological and materials characterization research endeavors.

Acknowledgments

The authors would like to thank Emanuele Cauda and Arthur L. Miller for their thorough review of this

manuscript and Jared Cumpston and Eleanor Wade for assistance with sampling of the nanomaterials, as well as Matthew G. Duling for assistance with measurements. Financial support of this project was provided by the US Government.

Declaration of interest: The authors report no conflict of interest. The authors alone are responsible for the content and writing of the paper.

References

Bartley D. 2001. Definition and assessment of sampling and analytical accuracy. Annals Occupat Hyg 45:357–364.

Bello D, Hsieh SF, Schmidt D, Rogers E. 2009. Nanomaterials properties vs. biological oxidative damage: Implications for toxicity screening and exposure assessment. Nanotoxicology 3:249–261.

Bermudez E, Mangum JB, Wong BA, Asgharian B, Hext PM, Warheit DB, Everitt JI. 2004. Pulmonary responses of mice, rats, and hamsters to subchronic inhalation of ultrafine titanium dioxide particles. Toxicolog Sci 77:347–357.

Boffetta P, Soutar A, Cherrie JW, Granath F, Andersen A, Anttila A, Blettner M, Gaborieau V, Klug SJ, Langard S, Luce D, Merletti F, Miller B, Mirabelli D, Pukkala E, Adami H-O, Weiderpass E. 2004. Mortality among workers employed in the titanium dioxide production industry in Europe? Cancer Causes Control 15:697–706.

Chen B, Frazer D, Stone S, Schwegler-Berry D, Cumpston J, McKinney W, Lindsley W, Frazer A, Donlin M, Vandestouwe K, et al. 2006. Development of a small inhalation system for rodent exposure to fine and ultrafine titanium dioxide aerosols. In: Biswas P, Chen D-R, Hering S, editors. Proceedings of the 7th International Aerosol Conference. American Association for Aerosol Research, St. Paul, MN. pp 858–859.

Donaldson K, Stone V, Gilmour PS, Brown DM, MacNee W. 2000. Ultrafine particles: Mechanisms of lung injury. Philosoph Transact: Math, Phys Engineering Sci 358:2741–2749.

Duffin R, Tran CL, Clouter A, Brown DM, MacNee W, Stone V, Donaldson K. 2002. The importance of surface area and specific reactivity in the acute pulmonary inflammatory response to particles. Annals Occupat Hyg 46:242–245.

Dwivedi PD, Misra A, Shanker R, Das M. 2009. Are nanomaterials a threat to the immune system? Nanotoxicology 3:19–26.

Ferin J, Oberdörster G, Penney DP. 1992. Pulmonary retention of ultrafine and fine particles in rats. Am J Respirat Cell Molec Biol 6:535–542.

Fryzek JP, Chadda B, Marano D, White K, Schweitzer S, McLaughlin JK, Blot WJ. 2003. A cohort mortality study among titanium dioxide manufacturing workers in the United States. J Occupat Environ Med 45:400–409.

Grieger K, Hansen S, Baun A. 2009. The known unknowns of nanomaterials: Describing and characterizing uncertainty within environmental, health and safety risks. Nanotoxicology 3:222–U17.

Hansen SF, Larsen BH, Olsen SI, Baun A. 2007. Categorization framework to aid hazard identification of nanomaterials. Nanotoxicology 1:243–250.

Hansen SF, Michelson ES, Kamper A, Borling P, Stuer-Lauridsen F, Baun A. 2008. Categorization framework to aid exposure assessment of nanomaterials in consumber products. Ecotoxicology 17:438–447.

Hussain S, Boland S, Baeza-Squiban A, Hamel R, Thomassen LCJ, Martens JA, Billon-Galland MA, Fleury-Feith J, Moisan F, Pairon JC and others. 2009. Oxidative stress and proinflammatory effects of carbon black and titanium dioxide nanoparticles: Role of particle surface area and internalized amount. Toxicology 260:142–149.

Kennedy ER, Fischbach TJ, Song R, Eller PM, Shulman SA. 1995. Guidelines for air sampling and analytical method development and evaluation, 95-117. Cincinatti: National Institute of Occupational Safety and Health. pp 1–98.

Ku B, Maynard A. 2005. Comparing aerosol surface-area measurements of monodisperse ultrafine silver agglomerates by mobility analysis, transmission electron microscopy and diffusion charging. J Aerosol Sci 36:1108–1124.

Lawless P, Rodes C. 1999. Maximizing data quality in the gravimetric analysis of personal exposure sample filters. J Air Waste Manage Assoc 49:1039–1049.

LeBlanc A, Moseley A, Chen B, Frazer D, Castranova V, Nurkiewicz T. 2010. Nanoparticle inhalation impairs coronary microvascular reactivity via a local reactive oxygen species-dependent mechanism. Cardiovasc Toxicol 10:27–36.

Lee KP, Henry NW, Trochimowicz HJ, Reinhardt CF. 1986. Pulmonary response to impaired lung clearance in rats following excessive TiO_2 dust deposition. Environ Res 41:144–167.

Lee KP, Trochimowicz HJ, Reinhardt CF. 1985a. Pulmonary response of rats exposed to titanium dioxide (TiO_2) by inhalation for two years. Toxicol Appl Pharmacol 79:179–192.

Lee KP, Trochimowicz HJ, Reinhardt CF. 1985b. Transmigration of titanium dioxide (TiO_2) particles in rats after inhalation exposure. Experim Molec Pathol 42:331–343.

Maier M, Hannebauer B, Holldorff H, Albers P. 2006. Does lung surfactant promote disaggregation of nanostructured titanium dioxide? J Occupat Environ Med 48:1314–1320.

Monteiller C, Tran L, MacNee W, Faux S, Jones A, Miller B, Donaldson K. 2007. The pro-inflammatory effects of low-toxicity low-solubility particles, nanoparticles and fine particles, on epithelial cells in vitro: The role of surface area. Occupat Environ Med 64:609–615.

Nurkiewicz T, Porter D, Hubbs A, Stone S, Chen B, Frazer D, Boegehold M, Castranova V. 2009. Pulmonary nanoparticle exposure disrupts systemic microvascular nitric oxide signaling. Toxicolog Sci 110:191–203.

Oberdörster G, Maynard A, Donaldson K, Castranova V, Fitzpatrick J, Ausman K, Carter J, Karn B, Kreyling W, Lai D, et al. 2005. Principles for characterizing the potential human health effects from exposure to nanomaterials: Elements of a screening strategy. Particle Fibre Toxicol 2:1–35.

Park E-J, Yoon J, Choi K, Yi J, Park K. 2009. Induction of chronic inflammation in mice treated with titanium dioxide nanoparticles by intratracheal instillation. Toxicology 260: 37–46.

Rothenberger SJ. 1980. Coal combustion fly ash characterization: Adsorption of nitrogen and water. Atmospher Environ 14: 445–456.

Scuri M, Chen B, Castranova V, Reynolds J, Johnson V, Samsell L, Walton C, Piedimonte G. 2010. Effects of titanium dioxide nanoparticles exposure on neuroimmune responses in rat airways. J Toxicol Environ Health A 73:1353–1369.

Seaton A, Tran L, Aitken R, Donaldson K. 2010. Nanoparticles, human health hazard and regulation. J R Soc Interface 7;Suppl 1: S119–129.

Sheffield A, Pankow J. 1994. Specific surface-area of urban atmospheric particulate matter in Portland, Oregon. Environ Sci Technol 28:1759–1766.

Singh S, Shi T, Duffin R, Albrecht C, van Berlo D, Hohr D, Fubini B, Martra G, Fenoglio I, Borm PJA, et al. 2007. Endocytosis, oxidative stress and IL-8 expression in human lung epithelial cells upon treatment with fine and ultrafine TiO_2: Role of the specific surface area and of surface methylation of the particles. Toxicol Appl Pharmacol 222: 141–151.

Stefaniak A, Hoover M, Dickerson R, Peterson E, Day G, Breysse P, Kent M, Scripsick R. 2003. Surface area of respirable beryllium metal, oxide, and copper alloy aerosols and implications for assessment of exposure risk of chronic beryllium disease. AIHA J 64:297–305.

Stoeger T, Reinhard C, Takenaka S, Schroeppel A, Karg E, Ritter B, Heyder J, Schulz H. 2006. Instillation of six different ultrafine carbon particles indicates a surface area threshold dose for acute lung inflammation in mice. Environ Health Perspect 114:328–333.

Trochimowicz H, Lee K, Reinhardt C. 1988. In vivo effects of nuisance dusts (1). J Appl Toxicol 8: 383–385.

Weibel A, Bouchet R, Knauth P. 2005. The big problem of small particles: A comparison of methods for determination of particle size in nanocrystalline anatase powders. Chem Materials 17:2378–2385.